

Synthesis and characterization of $Zn_{1-x}Mn_xO$ nanowires

Xiaomei Zhang,^{1,2} Yue Zhang,^{1,a)} Zhong Lin Wang,^{2,a)} Wenjie Mai,² Yudong Gu,² Wangsheng Chu,³ and Ziyu Wu³

¹Department of Materials Physics and Chemistry, State Key Laboratory for Advanced Metals and Materials, University of Science and Technology Beijing, Beijing 100083, People's Republic of China

²School of Materials Science and Engineering, Georgia Institute of Technology, Atlanta, Georgia 30332-0245, USA

³Beijing Synchrotron Radiation Facility, Institute of High Energy Physics, Chinese Academy of Sciences, Beijing 100049, People's Republic of China

(Received 7 February 2008; accepted 13 March 2008; published online 21 April 2008)

Mn doped ZnO nanowires (NWs) were fabricated by a one-step vapor-solid process at 500 °C. The doped Mn exists in the wurtzite lattice as substitutional atom without forming secondary phases. X-ray absorption near-edge structure reveals that the doped Mn atoms occupy the Zn sites, and they lead to an expansion in lattice constants. The *I-V* characteristic of a single $Zn_{1-x}Mn_xO$ NW shows a typical Ohmic contact with gold electrodes. The as-received NWs could be suitable for studying spintronics in one-dimensional diluted magnetic semiconductors. © 2008 American Institute of Physics. [DOI: [10.1063/1.2905274](https://doi.org/10.1063/1.2905274)]

Due to a high Curie temperature above 300 K as predicted by theoretical calculation, diluted magnetic semiconductors (DMSs) are regarded as important materials for spintronics.¹ Combining ferromagnetism and semiconductivity gives an additional degree of freedom and functionality for fabricating unique devices with applications ranging from nonvolatile memory to quantum computing.^{2,3} Synthesis methods such as chemical vapor deposition and pulse laser deposition have been developed to prepare DMS thin films.⁴⁻⁶ It is known that different synthetic methods result in variance in environment of doping element in the matrix or forming second phase.

Exploring one-dimensional (1D) DMS materials are of great interest because nanowires (NWs) and nanobelts are ideal materials for fabricating field effect transistors, sensors, optoelectronic devices, logic circuits, and lasers.⁷⁻¹¹ There are two approaches for receiving DMS NWs. One method is doping the as-synthesized NWs by ion implantation.¹² This is a postgrowth doping via physical method, which usually requires postannealing to reduce the defects created by ion implantation. Moreover, ion implantation usually results in a depth variation in doping concentration. The other approach is by incorporating doping elements in the precursors during growth, which is a methodology for receiving uniformly distributed doping element in the matrix.^{13,14} For the NWs synthesized by the second approach, a key question is if the doping element is incorporated into the volume lattice or at the surface. Establishing an effective approach for synthesizing volume-doped DMS NWs is of fundamental importance for investigating spin transport in 1D nanomaterials and fabrication of NW based spintronic devices.

In this letter, we used a vapor-solid process to synthesize Mn doped ZnO NWs. The electronic structure and near neighbor distribution around the Mn atoms have been investigated by x-ray absorption near-edge structure (XANES). The results confirmed that the Mn atoms have been doped into the lattice of ZnO NWs and the doping is substitutional.

The electric transport of a single $Zn_{1-x}Mn_xO$ NW has also been measured and a conductivity of $\sim 0.025 \Omega^{-1} \text{cm}^{-1}$ has been received.

Our synthesis was based on a vapor-solid process via thermal evaporation. High purity Zn powders (99.99%) and $MnCl_2 \cdot 4H_2O$ powders (99.99%) were used as source materials. The source materials were placed in an alumina boat that was placed at the center of a horizontal tube furnace. A silicon substrate was placed above the boat. The tube furnace was heated to 500 °C with a constant argon flow of 100 SCCM (SCCM denotes cubic centimeter per minute at STP). After 3 h, a yellowish layer was received on the silicon wafer. The color of the as-received sample is clearly different from the white color of conventional ZnO NWs.

The morphology and chemical composition of the as-synthesized sample were characterized by scanning electron microscopy (SEM). Figure 1(a) shows an SEM image of $Zn_{1-x}Mn_xO$ NWs, with uniform diameters and lengths up to 100 μm . From the typical TEM image of Mn doped ZnO NWs in Fig. 1(b), the average diameter of the NWs is ~ 60 nm. To precisely define the chemical composition of the NWs, we used energy dispersive x-ray spectroscopy (EDS) attached to a transmission electron microscope (TEM) (Hitachi HF-2000) to quantify the chemical composition of a single NW without the interference from the substrate. The Mn peak is clearly shown in the EDS spectrum [Fig. 1(b)] and the Mn content in the ZnO NW is determined to be ~ 4.8 at. %. This apparently indicates that the NW contains Mn.

The phase of the as-synthesized NWs is identified by x-ray diffraction (XRD). The result indicate that the as-received $Zn_{1-x}Mn_xO$ ($x=0.048$) NWs has the wurtzite structure (Fig. 2). No secondary phase was found from the XRD spectrum, thus, the doping element Mn must be incorporated into the lattice as substitutional atom. The doping causes significant change in lattice constants, resulting in measurable shift in the (10-10) and (0002) peaks (see the insets in Fig. 2), corresponding to an expansion in lattice constants by $\Delta a/a=0.59\%$, $\Delta c/c=0.5\%$ after doping.

^{a)} Authors to whom correspondence should be addressed. Electronic addresses: yuezhang@ustb.edu.cn and zlwang@gatech.edu.

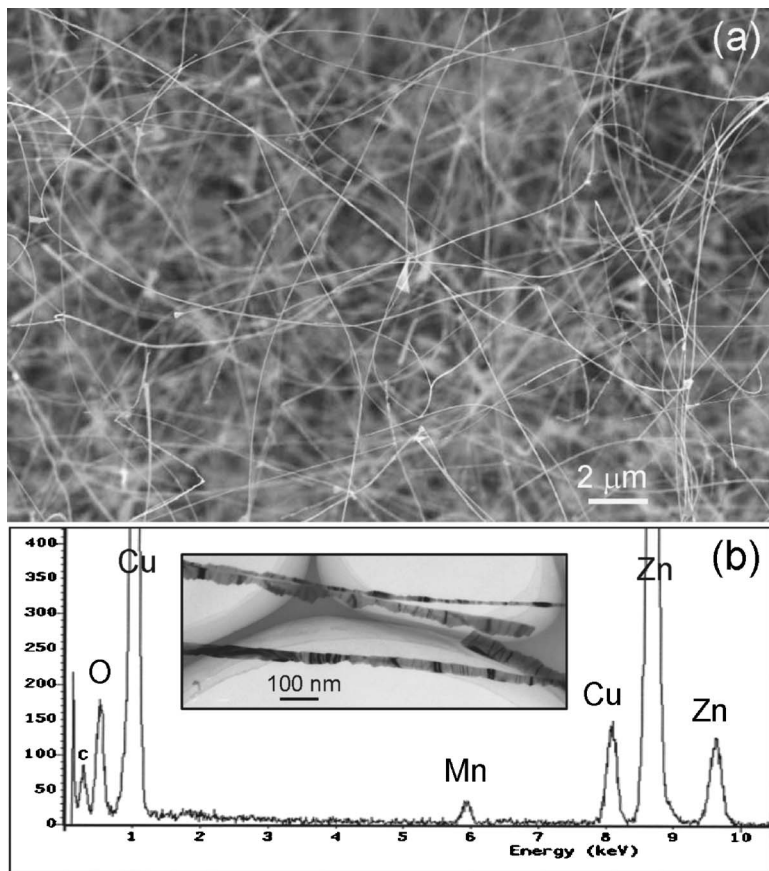


FIG. 1. (a) SEM image of $Zn_{1-x}Mn_xO$ NWs. (b) Typical EDX spectrum taken from individual $Zn_{1-x}Mn_xO$ NW in TEM, which gives that the Mn content is ~ 4.8 at. %. Inset in (b) is a TEM image of a 60 nm NWs with single crystal structure.

The occupation sites for the Mn dopants in the lattice are determined by XANES. The Mn K edge of the $Zn_{1-x}Mn_xO$ NWs [Fig. 3(a)] was measured in fluorescence yield mode by using synchrotron radiation with a silicon (111) double crystal monochromator at the x-ray absorption station (Beam line 1W1B) of the Beijing Synchrotron Radiation Facility (BSRF). The storage ring was operated at the typical energy of 2.5 GeV with the electron current decreasing from 200 to 100 mA in the span time of 12 h. XANES spectrum is very sensitive to the near neighbor distribution of atoms around the selected atom due to the multiple-scattering processes of the photoelectron emitted by the x-ray-absorbing

atom.^{15–17} The shoulder, main peak, and features at 10–90 eV beyond the Mn K edge of the $Zn_{1-x}Mn_xO$ are clearly different from those of standard samples such as Mn, MnO , Mn_2O_3 , and MnO_2 [Fig. 3(a)]. This excludes the possibility of Mn forming Mn clusters and other manganese oxides in the $Zn_{1-x}Mn_xO$ NWs. To find out the possibility of Mn substituting Zn in the lattice, the Mn K edge of the $Zn_{1-x}Mn_xO$ NWs is compared to the Zn K edge feature of ZnO at an energy of 10–90 eV beyond the edges [Fig. 3(b)]. The striking similarity between the XANES's from Mn K and Zn K edges reveals that the occupancy sites of Mn atoms in the $Zn_{1-x}Mn_xO$ NWs are the Zn sites. Therefore, the doped Mn atoms are in the volume of the NWs and they occupy the Zn sites.

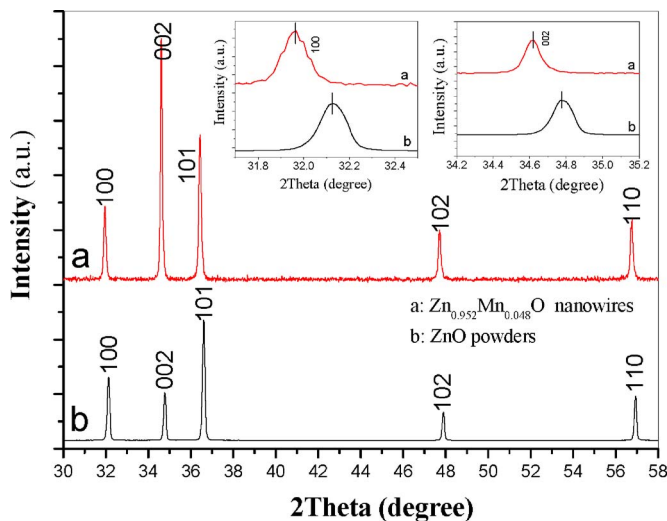


FIG. 2. (Color online) [(a) and (b)] XRD patterns of $Zn_{1-x}Mn_xO$ NWs and standard ZnO powders, respectively. The insets are the enlarged (100) [or (10-10)] and (002) [or (0002)] diffraction peaks.

The doping element is likely to affect the transport property of the NWs. We have fabricated two-electrode bridged devices using individual NWs, and their transport properties have been measured. Figure 4 gives the I - V characteristic of a NW based device, in which a $Zn_{1-x}Mn_xO$ NW was in contact with two gold electrodes. The NW was laid on prefabricated electrodes by dielectrophoresis. To reduce the contact resistance, Pt was deposited at the contacts using a focused ion beam microscope (FEI Nova). An SEM image of the device is shown as the inset in Fig. 4. The I - V curve shows an Ohmic behavior of the NW, from the slope of which and the diameter and length of the NW measured from the SEM image, the conductivity of the $Zn_{1-x}Mn_xO$ NW is measured to be $\sim 0.025 \Omega^{-1} \text{cm}^{-1}$.

In conclusion, Mn doped ZnO NWs were fabricated by a one-step vapor-solid process at 500 °C. XANES reveals that the doping elements occupy the Zn sites. Electrical measurement on individual Mn-doped ZnO NW showed that Au electrodes made good Ohmic contacts with the $Zn_{1-x}Mn_xO$

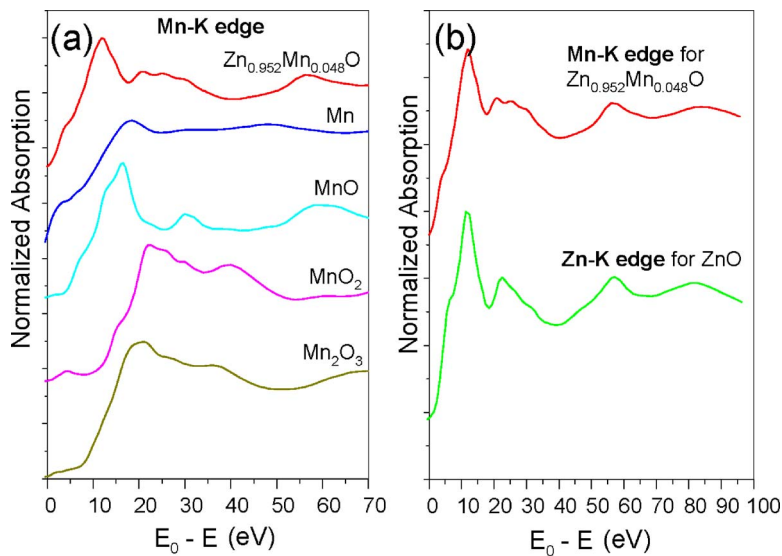


FIG. 3. (Color online) (a) Mn *K*-edge XANES spectra for $\text{Zn}_{1-x}\text{Mn}_x\text{O}$ NWs, Mn, MnO, Mn_2O_3 , and MnO_2 standards, respectively. (b) Mn *K*-edge XANES spectrum of $\text{Zn}_{1-x}\text{Mn}_x\text{O}$ NWs and the Zn *K*-edge XANES spectrum of ZnO.

NW. The as-received NWs could be suitable for studying spintronics in 1D DMS.

Thanks to Changshi Lao and Yong Ding at Georgia Institute of Technology (Atlanta, USA) for helping with the FIB and TEM experiments. This work was supported by the Major Project of International Cooperation and Exchanges (Nos. 50620120439 and 2006DFB51000), the National Basic Research Program of China (No. 2007CB936201), the National Natural Science Foundation of China (No. 50772011),

USA DOE BES (DE-FG02-07ER46394), and NSF (DMS 0706436).

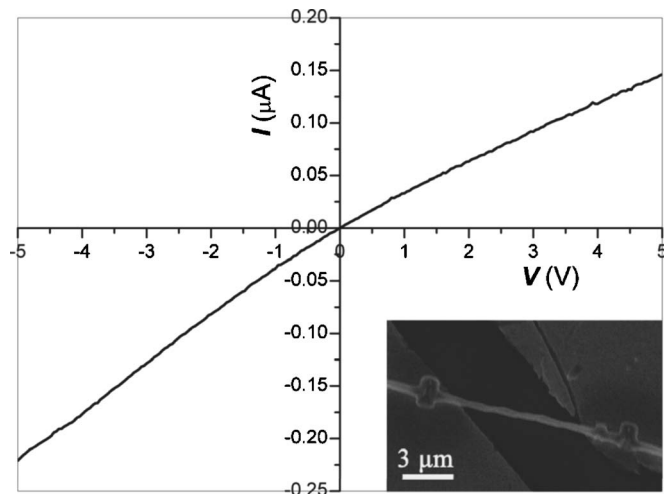


FIG. 4. *I*-*V* curve of a single $\text{Zn}_{1-x}\text{Mn}_x\text{O}$ NW. The inset shows an SEM image of a single NW contacted with two gold electrodes.

¹T. Dietl, H. Ohno, F. Matsukura, J. Cibert, and D. Ferrand, *Science* **287**, 1019 (2000).

²H. Ohno, *Science* **281**, 951 (1998).

³S. A. Wolf, D. D. Awschalom, R. A. Buhrman, J. M. Daughton, S. von Molnár, M. L. Roukes, A. Y. Chtchelkanova, and D. M. Treger, *Science* **294**, 1488 (2001).

⁴Q. Wan, *Appl. Phys. Lett.* **89**, 082515 (2006).

⁵Q. Xu, H. Schmidt, L. Hartmann, H. Hochmuth, M. Lorenz, A. Setzer, P. Esquinazi, C. Meinecke, and M. Grundmann, *Appl. Phys. Lett.* **91**, 092503 (2007).

⁶W. Yan, Z. Sun, Q. Liu, Z. Li, T. Shi, F. Wang, Z. Qi, G. Zhang, and S. Wei, *Appl. Phys. Lett.* **90**, 242509 (2007).

⁷Y. Nakayama, P. J. Pauzauskie, A. Radenovic, R. M. Onorato, R. J. Saykally, J. Liphardt, and P. D. Yang, *Nature (London)* **447**, 1098 (2007).

⁸S. J. Pearton, D. P. Norton, K. Ip, Y. W. Heo, and T. Steiner, *Prog. Mater. Sci.* **50**, 293 (2005).

⁹S. N. Cha, J. E. Jang, Y. Choi, G. A. J. Amaratunga, G. W. Ho, M. E. Welland, D. G. Hasko, D. J. Kang, and J. M. Kim, *Appl. Phys. Lett.* **89**, 263102 (2006).

¹⁰Z. L. Wang, *Adv. Mater.* **19**, 889 (2007).

¹¹Z. L. Wang, *Mater. Today* **10**, 20 (2007).

¹²C. Ronning, P. X. Gao, Y. Ding, Z. L. Wang, and D. Schwen, *Appl. Phys. Lett.* **84**, 783 (2004).

¹³J. J. Liu, M. H. Yu, and W. L. Zhou, *Appl. Phys. Lett.* **87**, 172505 (2005).

¹⁴H. L. Yan, X. L. Zhong, J. B. Wang, G. J. Huang, S. L. Ding, G. C. Zhou, and Y. C. Zhou, *Appl. Phys. Lett.* **90**, 082503 (2007).

¹⁵Z. Wu, A. Marcelli, A. Mottana, G. Giuli, E. Paris, and F. Seifert, *Phys. Rev. B* **54**, 2976 (1996).

¹⁶Z. Y. Wu, G. Ouvrard, P. Gressier, and C. R. Natoli, *Phys. Rev. B* **55**, 10382 (1997).

¹⁷Z. Wu, D. C. Xian, C. R. Natoli, A. Marcelli, E. Paris, and A. Mottana, *Appl. Phys. Lett.* **79**, 1918 (2001).